


Article

# Investigation of Partial Discharges within Power Oil Transformers by Acoustic Emission

Franciszek Witos \*  and Aneta Olszewska 

Department of Optoelectronics, Faculty of Electrical Engineering, Silesian University of Technology,  
44-100 Gliwice, Poland

\* Correspondence: franciszek.witos@polsl.pl

**Abstract:** This paper presents the authors' multi-channel measurement systems designed and built to conduct research on partial discharge phenomena using the acoustic emission method. The systems provide real-time monitoring, recording of signals and analysis of recorded signals. The analysis is carried out in time, frequency, time-frequency and discrimination threshold domains. In particular, a descriptor with the ADC acronym is defined, which ranks the signals according to the so-called degree of advancement. Studies have been carried out, showing that for a single partial discharge source, when tested in parallel, using the electrical and acoustic emission methods, the ranking of the signals using this descriptor is identical to the ranking according to the value of the apparent charge introduced by sources. This paper presents the authors' patented method of partial discharge location and identification in power oil transformers. The results of tests of power oil transformer at the test station, conducted in parallel with the electric method and the authors' method, and the results of tests in three selected transformers carried out during ongoing in-situ operation using the authors' method are presented. Based on these results, the authors make diagnoses of the condition of the insulation systems in the tested transformers. The inspections of these transformers confirm the diagnoses.

**Keywords:** acoustic emission; partial discharge; power oil transformers; multi-channel measurement systems; acoustic emission descriptors; location; identification of sources



**Citation:** Witos, F.; Olszewska, A. Investigation of Partial Discharges within Power Oil Transformers by Acoustic Emission. *Energies* **2023**, *16*, 3779. <https://doi.org/10.3390/en16093779>

Academic Editors: Carlos Miguel Costa and Pietro Romano

Received: 24 February 2023

Revised: 27 March 2023

Accepted: 24 April 2023

Published: 28 April 2023



**Copyright:** © 2023 by the authors. Licensee MDPI, Basel, Switzerland. This article is an open access article distributed under the terms and conditions of the Creative Commons Attribution (CC BY) license (<https://creativecommons.org/licenses/by/4.0/>).

## 1. Introduction

Partial discharges (PDs) are electrical discharges of a local nature, locally occurring in a dielectric located in an external electric field. They manifest an electrical nature and are revealed by the occurrence of a current pulse and the emission of an electromagnetic wave. PDs arise and develop according to various mechanisms. PDs are related to internal defects in the structure of the insulation system. These defects arise in the technological process and/or in operation as a result of various types of exposure (electrical, thermal, thermomechanical, etc.) [1–3].

The basic elements of the PDs' description are initiation, development and extinction. The initiation of PDs requires the fulfillment of the following conditions: (i) exceeding the critical electric field strength in the relevant dielectric region and (ii) the presence of free electrons in this region [4]. The development of PDs is associated with the formation and development of electron avalanches, leading to self-sustaining discharges ultimately giving rise to a streamer mechanism or streamer-leader mechanism.

The development of PDs leads to the degradation of the electrical strength of the dielectric, and in the case of power equipment, this creates a deterioration in the suitability of the insulation for continued operation, which can lead to damage to the insulating system of the power equipment. In electric power systems, power oil transformers are an important component. Their technical diagnostics in the area of researching PD phenomena are of an increasing practical importance for professional and industrial power engineering,

as an ongoing assessment of the technical condition of the insulation can be made on the basis of properly performed diagnostic tests. On this basis, a decision is made about its further operational suitability, including its transfer for repair or decommissioning.

PDs are accompanied by numerous groups of phenomena. They are mainly: chemical transformation of insulation, impact elastic deformation and the accompanying emission of acoustic emission waves, light radiation, local temperature changes and changes in gas pressure in the discharge channel. The first two groups of phenomena are of great importance for the description and assessment of PD. They are used in the gas chromatography method [5,6] and acoustic emission (AE) method [7,8].

It should be emphasized that due to the electrical nature of PD phenomena, the main role is played by electrical methods. Other methods are complementary methods, but in specific research conditions, after their calibration, they can play a very important role. This is the case, for example, in the area of PD research in power oil transformers, where research that can be carried out during the normal operation of the diagnosed device is preferred.

An example of such a method is the AE method, which has been dynamically developing in recent years. It is an important complement to the electrical method and the gas chromatography method. The AE method creates a unique opportunity to observe deformational processes, enabling non-invasive detection of PDs in power transformers, based on diagnostic measurements performed without the need to turn off the tested objects. In addition to information about the occurrence of PDs, the AE method allows the location of their sources. The AE method is gaining more and more importance in the measurement of PDs, as evidenced by research conducted in various research centers [7–14]. These are studies aimed at: (-) applications of the AE method in PD measurement in various power devices [7], (-) identification of different types of PDs by the AE method [8–10], (-) design and construction of AE measurement systems dedicated as online PD monitoring systems [11–14]

This paper concerns PDs in power oil transformers performed during the operation of transformers using the AE method.

In operating power oil transformers, there are many phenomena during which acoustic impulses are generated. These impulses are generated in areas of transformers where the sources of these phenomena occur. Then, they propagate in the volume of the transformer and reach the side walls of the transformer tank, where they can be recorded, in particular by the installed AE sensors. These phenomena are:

- (a) acoustic emission (AE) signals generated during deformational processes that accompany partial discharges (PDs) [8,9,13–15],
- (b) magnetoacoustic emission signals generated by numerous phenomena that occur during the magnetization of the ferromagnetic materials [16,17],
- (c) acoustic signals generated during oil circulation in the transformer [18],
- (d) vibroacoustic signals [18,19],
- (e) outer acoustic interference.

This multiplicity of phenomena giving acoustic signals makes it difficult to register only the AE signals generated during deformational processes that accompany PDs.

The main frequency band for AE signals generated during deformational processes that accompany PDs in power oil transformers is approximately from 20 kHz to 50 kHz, but these signals have additional frequency bands above 100 kHz [10,11,14].

The analysis of the main signal bands for the phenomena listed in points (b)–(e) leads to the conclusion that the total frequency band for these phenomena reaches approximately 100 kHz.

Thus, the analysis of the recorded acoustic signals above 100 kHz provides filtering of the signals from the phenomena mentioned in (b) to (e) and the signal after such filtering is the AE signal generated during deformational processes that accompany PDs. This is one of the assumptions of the authors' method for PD testing in power oil transformers by using the AE method.

This paper presents the authors' multi-channel measurement systems designed and built to conduct research on PD phenomena using the AE method. The systems provide real-time monitoring and recording of signals as well as analysis of recorded signals. The analysis of the recorded AE signals is carried out in the time, frequency, time-frequency and discrimination threshold domains. In particular, the AE descriptor with the acronym ADC has been defined in the domain of the discrimination threshold. This descriptor ranks the signals according to the so-called degree of advancement. Studies, using parallel tests by the electrical method and the AE method, have been carried out showing that for a single source of PDs, the ordering of signals using the ADC descriptor is identical to the ordering of PD sources according to the value of the introduced apparent charge.

This paper presents the authors' patented method of localization and identification of PDs in power oil transformers. This method is verified during PD tests in a power oil transformer at the test station, where the tests are carried out in parallel with the electric method and the authors' AE method. Then, the method is applied to the tests of 10 power oil transformers during their operation. This paper presents the results of three selected transformers along with the diagnoses made by the authors. The inspections of these transformers confirm the diagnoses made by the authors. This work is a summary of the authors' previous research in the field of PDs in oil-filled power transformers using the AE method.

## 2. Measuring Systems for Acoustic Emission Signals

This research was carried out using two authors' measurement systems dedicated to the measurement of AE signals. The first was the four-channel DEMA-COMP system; the second was the eight-channel 8AE-PD system [20,21]. Both systems enable: (-) monitoring of signals in the selected measurement channel, (-) simultaneous recording of signals in all measurement channels in real time, providing in each measurement channel a bandwidth of 20–500 kHz (DEMA-COMP) or 25–1000 kHz (8AE-PD), respectively, under both laboratory and real conditions, (-) analysis of the recorded signals.

The block diagram of the designed and constructed mobile 8AE-PD measurement system together with AE sensors is shown in Figure 1. The system has the following properties: (-) built of modern sub-assemblies; (-) equipped with 8 measurement channels; (-) amplification within each channel is fully controlled in a program way and has 65 dB, dynamic of change of the input signal; (-) provides a wide range of frequencies of recorded signals (from 25 kHz to 1000 kHz); (-) the software operates in the LabVIEW environment and ensures the monitoring of signals, registration of data in real time (within a band of 25–1000 kHz) and analysis of recorded signals; (-) supplied from the power network 230 V/50 Hz.

The system consists of 8 preamplifiers, a main unit and a computer. The preamplifiers are separate elements of the measurement system and have been constructed to fulfil the tasks of amplifying signals coming from AE sensors and to secure the proper input impedance, stability and capability to eliminate disturbances. The main unit is constructed of the 8 measuring amplifiers, the system for formation of a reference signal, a 2560 ATMEGA microcontroller and a complete PXI 1033 chassis. This chassis contains a PXI 6133 measurement card together with a power supply and an integrated MXI-Express controller mounted inside of one casing. The PXI 6133 measurement card enables the processing of 14-bit samples with a speed of 2.5 MS/sec in each of the 8 channels. The MXI—Express interface ensures communication with the computer. The software written in LabVIEW environment enables the controlling of the measurement card and the inside microcontroller and programs for the monitoring of signals, registration of data and data analysis of registered signals. An additional notebook is equipped with a PCMCIA PXI Express Card 8360 from National Instruments. The data from the card transmitted to the computer are written in proper sets on the hard disc. A detailed description of the 8AE-PD measurement system is available in [20].

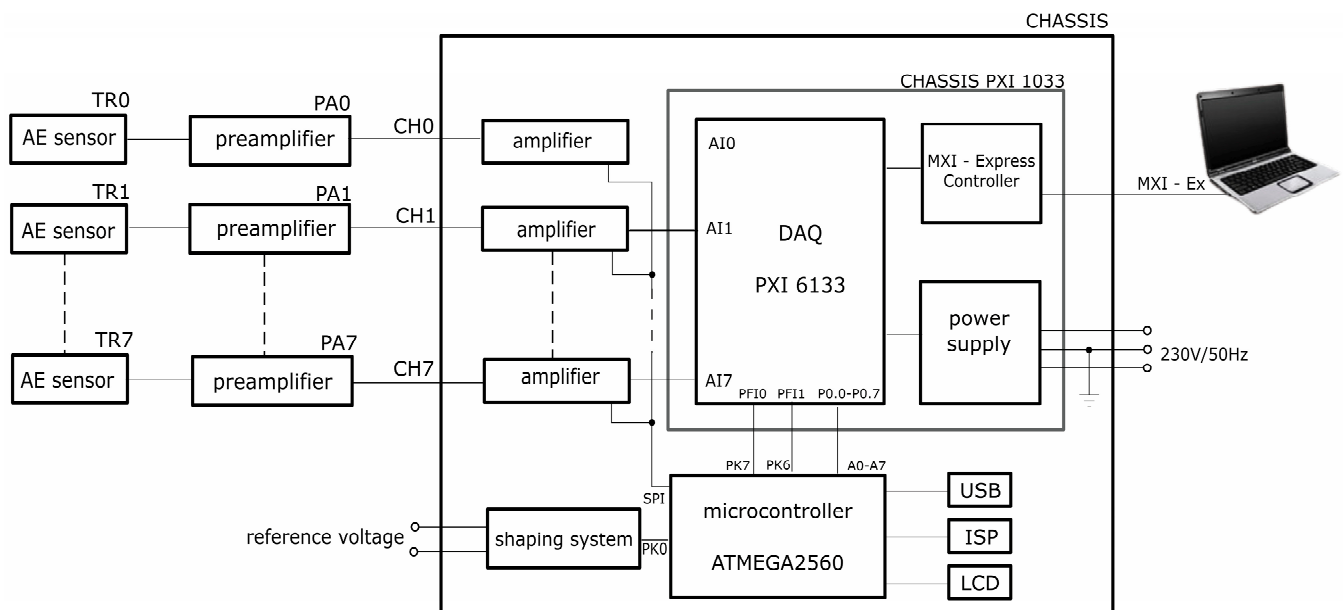


**Figure 1.** A block scheme of the 8AE-PD measurement system together with AE sensors.

During this research, the following sensors from Physical Acoustics Corporation were used: D9241A, WD, WDI and R6. As during the tests using the AE method, stability and an appropriate quality of assembly of AE sensors are required, which is why the authors designed and made housings for the AE sensors used in this research [22]. Photos of the AE sensor in the housing and the preamplifier as well as the preamplifier and AE sensors fastened to the wall of the tank of a laboratory model of transformer are presented in Figure 2a,b. For signals recorded in the measurement channel of 8AE-PD containing a resonance AE sensor of D9241A type, it is possible to identify the signal generated by a modeled PD source introducing an apparent charge with a value of 20 pC [21].

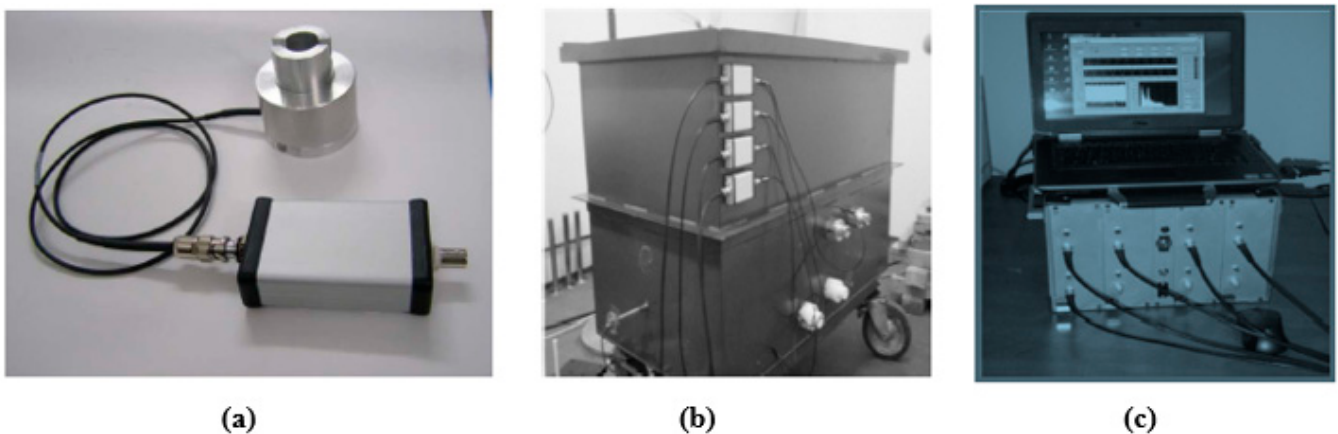


**Figure 2.** Photos of: (a) the AE sensor in the housing and the preamplifier; (b) the preamplifiers and AE sensors fastened to the wall of the laboratory tank; and (c) the main unit of the 8AE-PD measurement system with cables leading to the preamplifiers and computer.

### 3. Authors' Research Methods

#### 3.1. Analysis of Recorded Acoustic Emission Signals

This research covers the phenomena of PDs generated by modeled sources or generated in power devices when they are supplied with alternating high voltage. Due to the periodic and stochastic nature of these phenomena, signals with a duration of two seconds (approximately 100 periods of the supply voltage) are recorded each time.



In order to analyze the recorded signals, a system was built in the LabVIEW environment to provide analysis in the following domains: time, frequency, time-frequency and discrimination threshold. The results of the analysis for the selected signal recorded during the PD tests coming from the modeled source are presented in Figures 3 and 4.

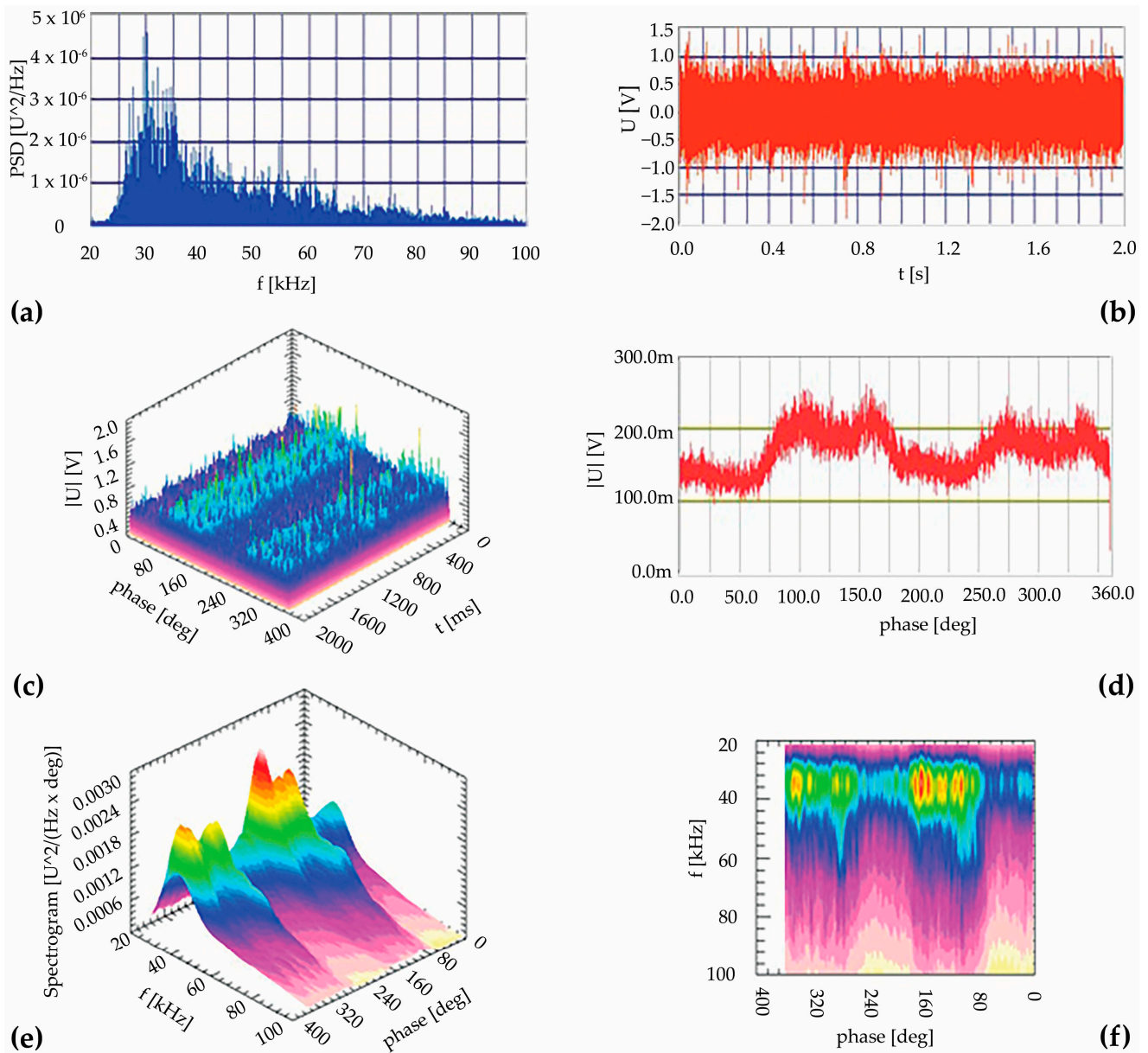


**Figure 3.** The results of the analysis of the AE signal recorded in measuring conditions: bushing with the end including the thread, 123 kV, 500 pC, measuring line with AE sensor of R6 type within (a) frequency domain, (b–d) time domain, (e,f) time-frequency domain: (a) signal power spectral density, (b) signal after filtering, (c) amplitude-phase-time characteristics, (d) averaged amplitude-phase characteristics, (e) averaged three-dimensional STFT spectrogram, (f) projection of the spectrogram from (e) to the phase-frequency plane.

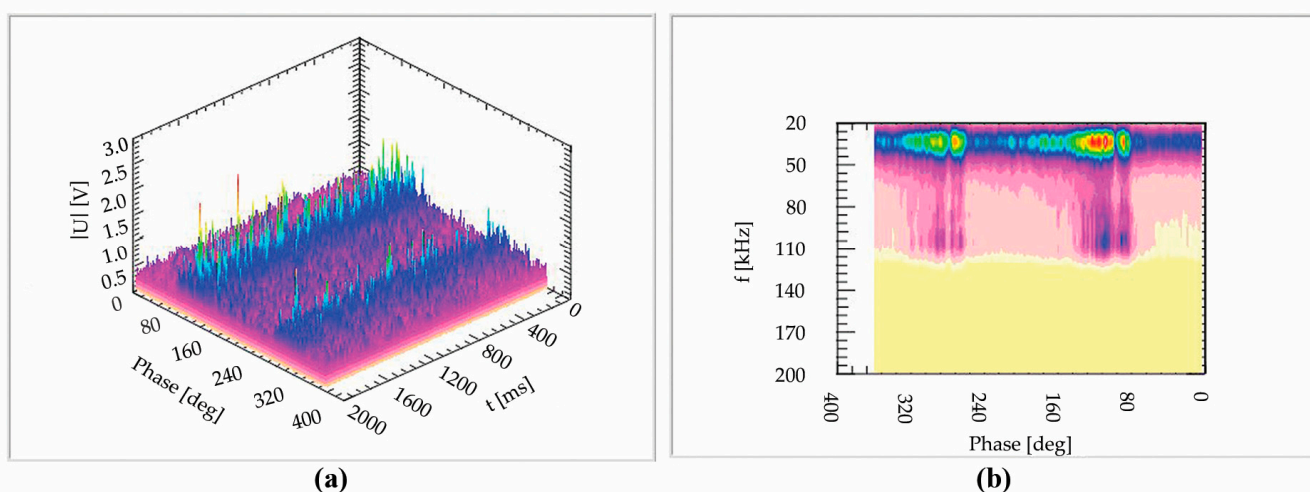


**Figure 4.** The results of the analysis of the AE signal recorded in measuring conditions: bushing with end with thread, 123 kV, 500 pC, measuring line with AE sensor of R6 type: (a) amplitude-phase-time characteristics, (b) averaged three-dimensional STFT spectrogram.

### 3.1.1. Analysis in Time, Frequency and Time-Frequency Domains

Figure 3 shows the results of signal analysis in the frequency (Figure 3a), time (Figure 3b–d) and time-frequency (Figure 3e,f) domains. These characteristics are obtained as follows:

- The frequency band for which the signal properties will be analyzed is determined (the selected band is visible as an independent variable in Figure 3a);
- the signal is filtered using a 5th order bandpass filter;
- For the filtered signal, the Fourier transform is calculated and the result in the spectral form of the power density for the signal is shown in Figure 3a, in the description of Figure 3a there are the frequency for the main maximum and the spectrum value for this frequency; the main band can be read from the graph signal;
- Figure 3b shows the filtered signal with the following values: minimum, maximum and RMS of the signal. The difference between the minimum and maximum values allows the calculation of the peak-to-peak voltage of the signal, i.e.,  $U_{pp}$ ;
- Figure 3c shows the amplitude-phase-time characteristic, which is obtained in the following way: (a) the filtered signal is divided into fragments in relation to the periods of the reference voltage, (b) for each of these fragments the signal modulus is calculated; the signal module is marked in Figure 3c as “ $|U|$  [V]”, (c) these moduli of the signal fragments are placed on the amplitude-phase-time characteristic as ‘two-dimensional sections’, (d) the amplitude-phase-time characteristics of the signal are created by “stitching” such “two-dimensional sections” and (e) for a periodic signal “tunnels” are visible, which illustrate the periodic nature of the recorded data;
- Figure 3d shows the averaged amplitude-phase characteristic of the signal module; it is created by averaging all “two-dimensional cross-sections” with respect to the phase of the reference voltage;
- The analysis in the time-frequency domain is based on the Joint Time-Frequency Analysis by National Instruments [23]; the basis is the calculation of the Short-Time Fourier Transform (STFT) spectrogram for successive signal fragments with a length of one period of the reference voltage;
- Figure 3e shows a three-dimensional STFT spectrogram, which is obtained by averaging
- The three-dimensional STFT spectrograms calculated for all signal fragments; the three-dimensional STFT spectrogram is marked in Figure 3e as “spectrogram [ $V^2/(Hz \times deg)$ ]”;
- Figure 3f shows a two-dimensional STFT spectrogram which is obtained after projecting the STFT spectrogram of Figure 3e onto the phase-frequency plane.

The results of the analysis of the AE signals originating from the acoustic phenomena accompanying the PDs presented in the graphs in Figure 3 give a lot of information about the recorded signals. This information is related to the properties of the PDs' sources.

In particular, the amplitude-phase-time characteristic and the averaged three-dimensional STFT spectrogram are significant. The "tunnels" visible in Figure 3c indicate the periodic nature of the studied phenomenon, while the fluctuations of the position of the "two-dimensional cross-sections" for individual signal fragments with a length of one reference voltage period describe the stochastic nature of the PD phenomena. These fluctuations in the value of the reference voltage phase for which the PD is initiated indicate, for example, different values of the charge (remaining after the extinguished PD) accumulated in the region of the initiated PD. On the other hand, the averaged three-dimensional STFT spectrogram is the most sensitive characteristic, allowing the authors to distinguish between different types of PDs.

The indicated description contains many parameters describing features of the selected signal recorded during the PD tests. The written software provides such an analysis for the entire recorded signal or for its selected fragment. It is worth adding that the recorded EA signals are the burst AE. Thus, when selecting a fragment of the recorded AE signal, the analysis shows new features of the registered pulses, such as rise time, duration, peak amplitude, energy and average frequency [24].

It should be added that PDs (in addition to the main signal band) have additional frequency bands above 100 kHz. This is confirmed by the works [10,11,14]. This is also seen in Figure 4, which shows an additional frequency band near 100 kHz. It should be added that this band lies outside the operating band of the R6 type resonant sensor, which means that the recorded signal in this band has significant harmonic components.

### 3.1.2. Analysis in the Discrimination Threshold Domain

In the analysis of AE signals in the discrimination threshold domain, basic AE descriptors are defined, such as counts ( $N$ —the number of AE signal exceeds threshold) and count rate ( $dN/dt$ —number of counts per time unit). These values are determined for the selected discrimination threshold  $U_d$  [24].

To describe the registered AE signals in the discrimination threshold domain, the authors use a self-defined descriptor with the acronym ADC. In order to calculate these descriptors, the authors create the amplitude distributions of the counts  $N(U_d)$  and the counting rate  $dN(U_d)/dt$ . These distributions are determined by multiple analysis of the recorded signals at different values of the discrimination threshold  $U_d$ .

Figure 5 shows the method of signal analysis in the domain of the discrimination threshold and the definition of the ADC descriptor.

Figure 5a shows the  $N(U_d)$  plot for the signal of Figure 3b; it is plotted on a logarithmic scale. For the value of the discrimination threshold in the  $[U_1, U_2]$  range, the graph is approximated by a fragment of a straight line. The slope of the approximated straight line is the new AE descriptor for this signal. The descriptor has been given an ADC (Amplitude Distribution of Count).

$$y_{approx}(U_d) = AU_d + B; A = ADC \quad (1)$$

The basic AE descriptors, i.e., counts and count rate, as well as the amplitude distributions of these descriptors, describe the recorded signal in the domain of the discrimination threshold.

When recording a signal using an AE sensor mounted on the surface of the medium in which the elastic wave propagates, the amplitude of the recorded signal depends, for example, on the thickness of the coupling layer between the front surface of the sensor and the medium. Thus, all descriptors based on the value of the measured signal have limitations resulting from acoustic methods. The proposed ADC descriptor is not based on directly measured signal values and eliminates, for example, the influence of the thickness of the coupling layer. The descriptor takes negative values and gives the signals different values. We will consider, for example, the noise of the measurement track and some

deformational process as two different signals. For these signals we will calculate the amplitude distributions, we will designate ADC descriptors for them and then the ADC descriptor for noise will be smaller than for the deformational process.

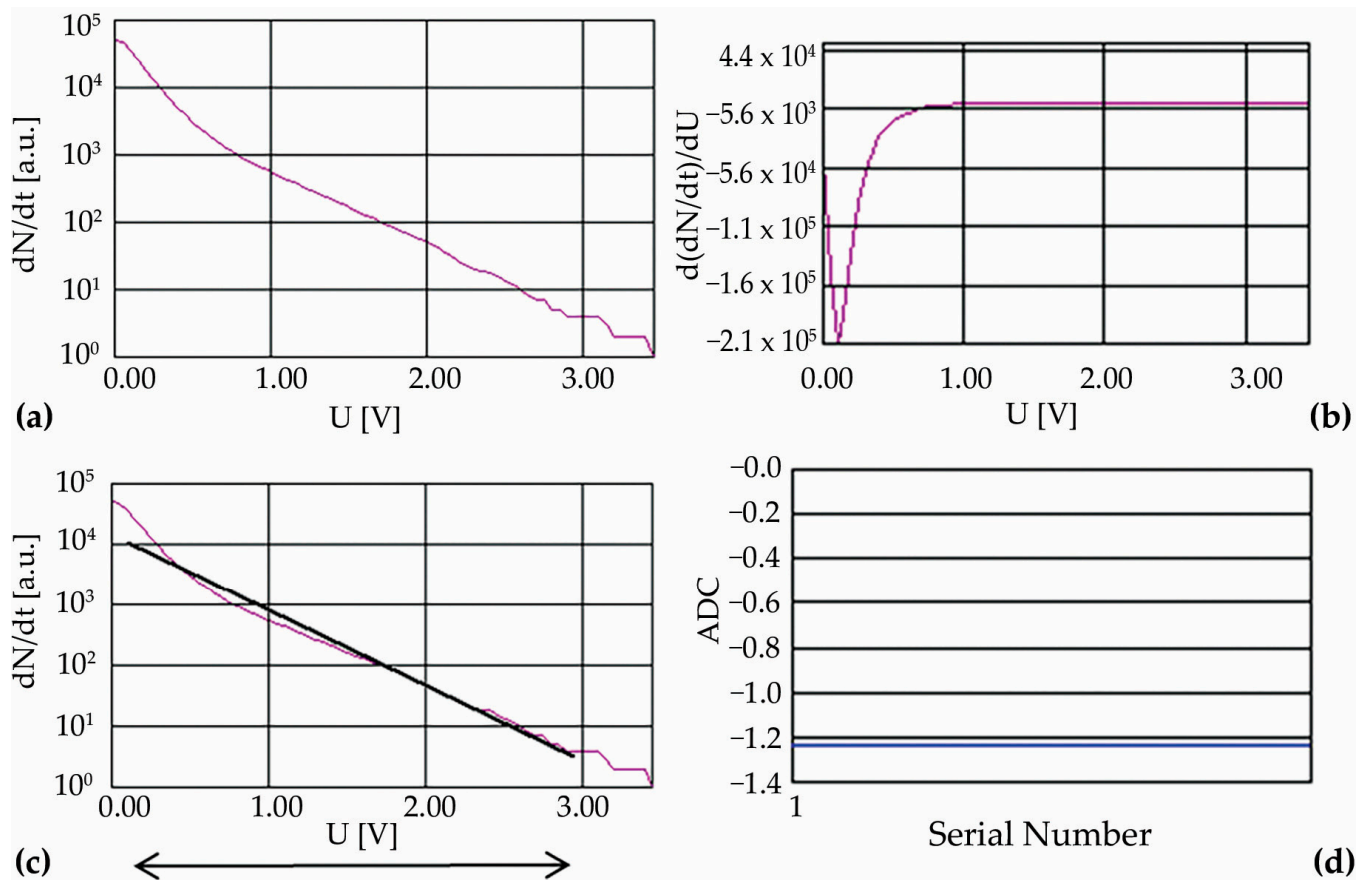


**Figure 5.** Calculation of ADC descriptor: (a) amplitude distribution of AE count of signal, (b) derivative of amplitude distribution of signal power, (c) amplitude distribution with approximation curve within the  $(U_1, U_2)$  range of threshold marked with the arrow and (d) ADC descriptor.

In Section 3.2 it is shown that for single PD sources, the ordering of the registered signals according to the ADC descriptor coincides with the ordering according to the value of the apparent charge introduced by the single sources. In Section 4 this descriptor property is used to analyze maps for the ADC descriptor values on the side walls of the tank of the tested transformers.

### 3.2. PDs Research in Systems with a Single Modelled Source—The Calibrated AE Method

The electrical method of PD measurement results from the electrical nature of PD phenomena and is the basic method of PD testing. The AE method provides the measurements of the acoustic phenomena accompanying PDs. If possible, it seems natural to carry out measurements in parallel with two methods, and then analyze and interpret the results obtained.

It is worth emphasizing that the results obtained by the electrical method characterize the entire tested object—therefore, they are global in nature. In turn, the results obtained with the AE method directly describe the signals recorded at a given measurement point of the object (they are local), and the connection of the AE signals with the AE pulses generated in the PDs sources requires knowledge of the propagation conditions of the AE pulses. In the case of a single source of PDs and simultaneous testing with the electrical method and the AE method, it is possible to calibrate the test results with the AE method based on the results of PD testing with the electrical method.



The modeled PD sources were built using a transformer bushing and making different bushing ends (end without additional elements, end with thread, end with a sharp). Such sources were placed individually in a modelled tank filled with oil. The studies of PD phenomena were carried out in parallel with two methods. In the electrical method, a PD measurement system type TE 571 by Haefely Trench was used, guaranteeing the fulfillment of the standards required for investigating PD phenomena [25]. In the AE method, the DEMA-COMP measurement system was used.

During the PD tests, the voltage value was changed and the value of the apparent charge introduced by the modelled source was determined using the electrical method, and the signals generated in the modelled source reaching the sensors mounted on the external surface of the tank were recorded using the AE method.

The results of the analysis of the recorded AE signal in the time, frequency and time-frequency domains for the selected measurement situation are shown in Figure 3. The characteristics presented in Figure 3 define the following important features of the recorded signal: the main band of the signal was from 20 kHz to 45 kHz, harmonics in the from 45 kHz to 60 kHz band are also visible, there are two “tunnels” (Figure 3c) on the amplitude-phase-time characteristics confirming the periodicity of the studied phenomena, the fluctuations of the shape of these “tunnels” show the random character of the studied phenomena and the time-frequency analysis (Figure 3e,f) confirms the main band, but at the same time shows and specifies the fluctuation of the frequency band for signals analyzed at different phases of the reference signal, giving for certain signals an extension of the band up to 60 kHz.

The results of the calculations of the properties of the registered AE signals in the domain of the discrimination threshold are summarized in Table 1.

**Table 1.** Results of apparent charge Q measurements (electrical method) and calculations of ADC descriptors for recorded signals (AE method). Result for following measuring conditions: bushing with the end without additional elements, bushing with sharp, bushing with thread.

No.	Q	ADC	No.	Q	ADC	No.	Q	ADC
1	0	−29.5	10	90	−24.4	19	450	−4.1
2	0	−31.1	11	100	−27.5	20	450	−3.7
3	0	−32.1	12	100	−27.5	21	500	−3.7
4	0	−30.1	13	220	−17.5	22	500	−3.7
5	0	−29.8	14	220	−17.1	23	890	−3.3
6	0	−30.2	15	280	−7.3	24	890	−3.2
7	25	−24.8	16	280	−7.3	25	1000	−2.7
8	25	−26.4	17	360	−4.4	26	1000	−2.7
9	90	−23.4	18	360	−5.1			

This Table 1 shows the calculated ADC descriptors for the recorded AE signals and the values of the apparent charge introduced by the modelled source measured in the same measurement situation. The apparent charge values are listed in ascending order. The increasing nature of the ADC descriptor as the apparent charge value increases can also be seen. It should be emphasized that the AE signals were recorded with multiple mountings of the AE sensor. The apparent charge introduced by the source ranks the PD sources, i.e., ranks the PD phenomena. The results from Table 1 show that the ADC classifies AE signals, and this classification is similar to the classification obtained by the electrical method. The results from Table 1 show that for a single PD source, electrical measurements provide a calibration of the AE results through the ADC descriptors of the AE signals. Such a calibration is of practical importance. However, it should be emphasized



that the results of such a calibration describe a given measurement situation and do not directly describe the source of the AE signal.

When describing the AE signal, it should be remembered that AE is understood as a physical phenomenon and the measurement method includes the following elements: source, propagation space, sensor and signal processing. Within this description, the pulse generated in the source is subjected to successive transformations during the propagation in the medium, during registration with the sensor and during processing of the recorded signal. Successive transformations can be described as time-invariant linear transformations. At each of these stages, the output signal  $y(t)$  is a convolution of the input signal  $x(t - \tau)$  with the impulse response of the system  $h(\tau)$ :

$$y(t) = \int_{-\infty}^{\infty} h(\tau)x(t - \tau)d\tau \quad (2)$$

This means that the Fourier transform of the output signal is the product of the Fourier transform of the input signal  $X(\omega)$  and the transfer function of the system  $H(\omega)$ :

$$Y(\omega) = H(\omega)X(\omega) \quad (3)$$

In summary, AE measurements and study of the AE signal do not give direct information about the AE pulse generated by the source. The results of the analysis of the recorded AE signal contain information about the AE pulse generated in the source, but after the pulse has been subjected to subsequent transformations.

#### 4. PD Research in Power Oil Transformers

##### 4.1. The Authors' AE Method of PDs Research in Power Oil Transformers

The analysis of acoustic phenomena occurring in power oil transformers, original multi-channel AE measurement systems, AT level 2 certificates held by the authors, their experience in PD testing under laboratory conditions and the conducted PD testing in oil power transformers became the basis for the AE method for PD testing developed by the authors in oil power transformers. This method has been patented [26]. The components of this method are: the authors' multi-channel AE measurement system, the construction of a network of measurement points on the side walls of the transformer's oil tank, mounting the AE sensors, checking the quality of the mounting of individual sensors using the Hsu-Nielsen method, analysis of the properties of the acoustic emission signals generated during the Hsu-Nielsen tests, data recording and determining the authors' maps of the descriptors on the side walls of the tested transformer, together with the location of the areas with increased acoustic emission activity and analysis of the properties of the acoustic emission signals recorded at the measurement points in areas identified as local maxima on the descriptor maps along with identification of the sources of the registered signals.

In practice, the network of measurement points on the side walls of the transformer tank is obtained in the following way: for a given transformer, along the horizontal direction of the tank, possible locations of the measurement points are selected (the distance between the points is approximately 50–70 cm); the locations along the vertical direction differ by 50 cm. Coordinates (X,Y) in centimeters are assigned to individual points on the side walls of the tested transformers. The X-positions running along the transformer tank are: 0—the point being the center of the tap changer (TC), positive X values—for TC and then for the part of the tank from the high voltage bushing side (HVbs) until the point opposite the center of the TC, X negative values—for TC and then for the part of the tank from the low voltage bushing side (LVbs). The Y-height is running up the tank (0—bottom of the tank). The sketch of the oil power transformer with a tap changer (TC), and L1, L2, L3 phases is presented on Figure 6.

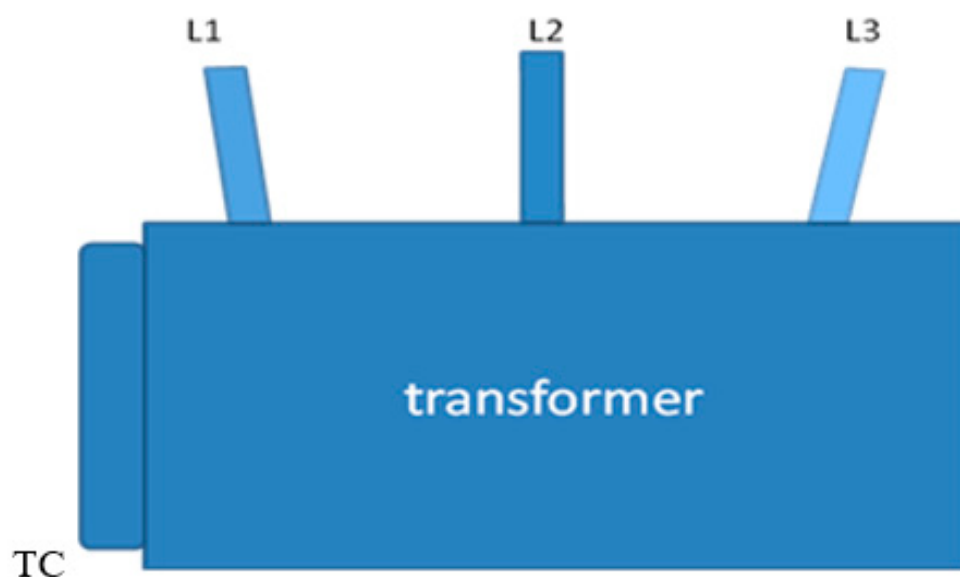


**Figure 6.** Sketch of oil power transformer with tap changer (TC), and L1, L2 and L3 phases.

Mounting the AE sensors and checking the quality of the mounting of individual sensors and array of sensors is performed in accordance with the requirements of the EN 14584:2013-07 Standard [27]. These requirements ensure the repeatability of the sensor system assembly process. During the research, as a base, AE sensors of the D9241A type are used as they provide high common noise rejection and low noise, even in electrically noisy environments. In addition, at measurement points where signals with high activity are recorded, WD and WDI type broadband sensors are installed. This stage of research is presented in detail in [28]. At each measurement point, AE signals are recorded several times; each of them has a length of 1 s. For each of the recorded signals, the ADC descriptor is calculated and finally, the average value of the ADC descriptors of all signals recorded in one measurement point is calculated. Calculated ADC values are input data to the descriptor map.

The next stage of the research is to create a map for the average ADC descriptor values on the side walls of the tank of the tested transformer within the frequency band from 110 kHz to 200 kHz. This map is created using the kriging method. The input data for the creation of the map are the calculated average ADC descriptor values at the measurement points of the grid.

On the created map, local maxima are located and the identification of PD sources is performed for AE signals registered at measurement points located in localized areas with high AE activity.

In order to confirm the correctness of the authors' proposed method, tests of the first transformer were carried out at the test station in parallel using the electrical method and the AE method.

After obtaining a positive result, 11 transformers were tested during their ongoing in-situ operation—only with the AE method. This paper presents the results of tests of three selected oil power transformers using the AE method, in which the occurrence of PD was found. These tests were carried out during ongoing in-situ operation. The sources of these PDs were located, and in two cases it was recommended to revise or repair these objects. The results of the revision confirm the correctness of the location of PD sources.

Tests of power oil transformers are tests in electrically noisy environments; therefore, in order to ensure the correct course of measurements and, consequently a proper analysis of the recorded signals, it is necessary to reduce the effect of noise and interference coming from the power grid. For this purpose, the authors used D9241A sensors. These sensors have very good EMI shielding ability and provide a high common noise rejection and low noise, even in electrically noisy environments. At the same time, during the research, the

authors took care of proper common grounding of all elements of the measuring system and the transformer.

In the overwhelming majority of cases, conducting the tests in this way ensured a good elimination of noise and interference from the power grid. For one tested transformer, unfortunately, the interference coming from the power grid was too large—then an additional solution in the form of isolating the measurement system by using an independent, own power supply was necessary.

#### 4.2. Parallel Research by the Electric Method and the AE Method

The first investigated object was a new 25 MVA, 220 kV transformer. During the test start-up at  $1.7 U_R$  ( $U_R$ —rated voltage) the PD tests with the electrical method show the presence of PDs sources introducing an apparent charge of 1 nC. This value is many times higher than the permissible level of PDs. Additional research was carried out using the AE method using the triangulation method to locate the sources—unfortunately, this method failed to locate the sources of PDs.

There was a need to use the AE method, in which there is a different type of location of PD sources. As the method proposed by the authors has such features, the authors undertook conducting this research. The tests were carried out in parallel with two methods, i.e., the electrical method and the AE method. The research had two stages. In the first stage, the transformer was supplied with a rated load of  $1.0 U_R$ . In the second stage, the voltage was increased to  $1.7 U_R$ .

The following results were obtained using the electrical method:

- for rated voltage, i.e.,  $1.0 U_R$ : none of the PD sources are detected in the case of the L1 phase; weak sources of surface charges have been stated in the L2 and L3 phases with levels of apparent charge 150 and 100 pC, respectively, allowable for the insulation system of the transformer,
- for voltage  $1.7 U_R$ : no PD sources are noted by first 1.5 h but later an apparent charge of 1 nC is measured in each of the phases.

The results of the analyses obtained with the AE method are shown in Figures 7 and 8 (for the voltage of  $1.0 U_R$ ) and Figures 9 and 10 (for the voltage of  $1.7 U_R$  after more than 1.5 h).

In Figure 7, on the ADC descriptor map, there are no PD sources in the L1 phase area and there are single PD sources in the L2 and L3 phase areas—the registered signals have descriptors with small values. The properties of the characteristics shown in Figure 8 identify the signal as coming from PD.

The descriptor map in Figure 9 shows that signals with large or very large ADC descriptor values are recorded over large areas of the side walls of the transformer tank. They occur mainly in the upper part of the transformer. For TC, they also occur in the lower parts, where connections from individual phases L1, L2 and LC are connected to TC. The characteristics presented in Figure 10, calculated for the signal recorded in the measurement point located in the AE-2 area, are not periodic in the signal phase; they have harmonics in the analyzed band from 110 kHz to 200 kHz. The latter fact confirms that these are signals coming from PDs.

From this research, the authors draw the following conclusions:

- the absence of PDs in the transformer for the rated voltage, i.e.,  $1.0 U_R$ , indicates the good condition of the insulation system in the transformer,
- the occurrence of PDs only after a longer time from the application of the voltage  $1.7 U_R$  in the areas visible in Figure 8 and the lack of periodicity of the signal in relation to the phase of the supply voltage leads the authors to put forward the following hypothesis:

“as a result of a longer transformer operation time, heating of the transformer takes place, which causes the oil temperature to rise, then gassing processes occur

in the used oil, creating “gas bubbles”; in the thus formed “gas bubbles” in those areas of the oil where the conditions for PDs initiation are fulfilled, PDs occur”.

Following this hypothesis, the owner of the transformer disclosed the fact that the transformer is filled with synthetic oil, which is currently undergoing testing to be released for operation. The oil has been removed and the transformer has been cleaned and filled with certified oil. Retesting by the electrical method at a voltage of  $1.7 U_R$  gave results similar to those obtained at a voltage of  $1.0 U_R$ .

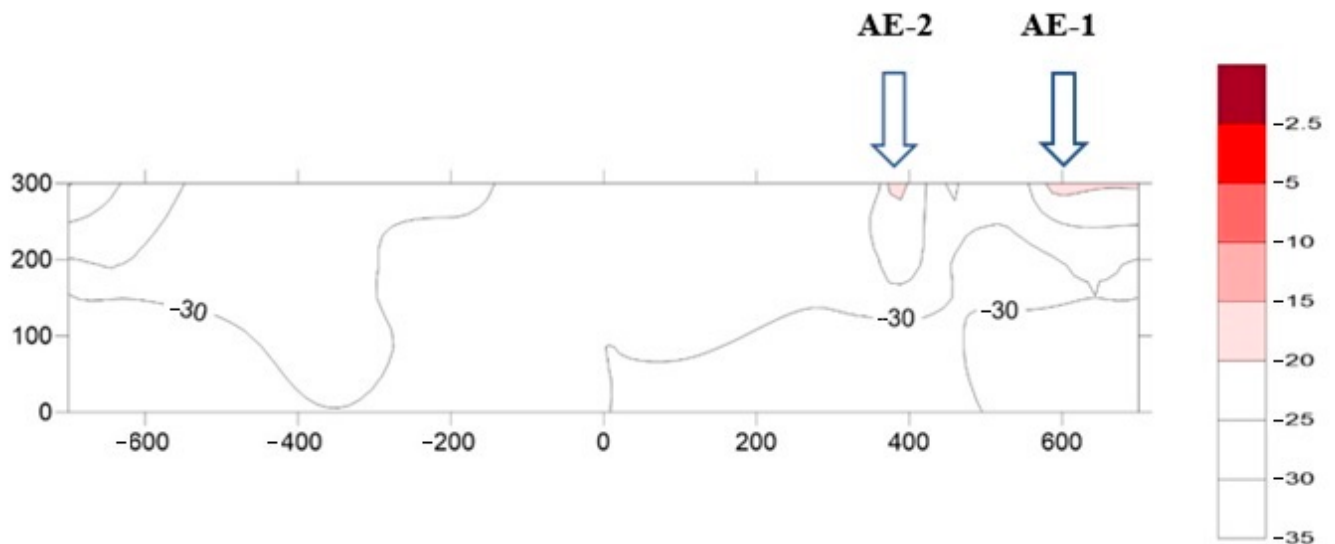


**Figure 7.** Map for the ADC descriptor values on the side walls of the tank of the tested transformer T1 with supply voltage  $1.0 U_R$  within the frequency band from 110 kHz to 200 kHz. The X-positions run along the transformer tank (0—the point being the center of the tap changer (TC), positive X values—for TC and then for the part of the tank from the high voltage bushing side (HVbs) until the point opposite the center of the TC, X negative values—for TC and then for the part of the tank from the low voltage bushing side (LVbs). Y-height runs up the tank (0—bottom of the tank).

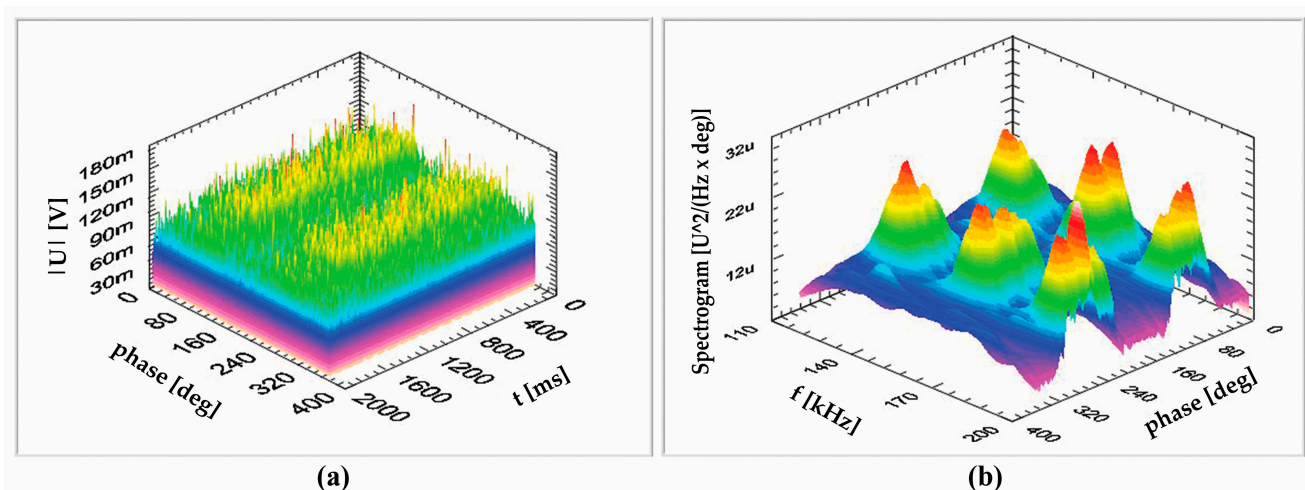


**Figure 8.** Acoustic image of a selected AE signal from AE-2 area within the Figure 7: (a) amplitude-phase-time characteristics, (b) averaged three-dimensional STFT spectrogram. AE signal parameters: ADC =  $-18.05$ ,  $U_{pp} = 0.29$  V,  $U_{rms} = 9.25$  mV.

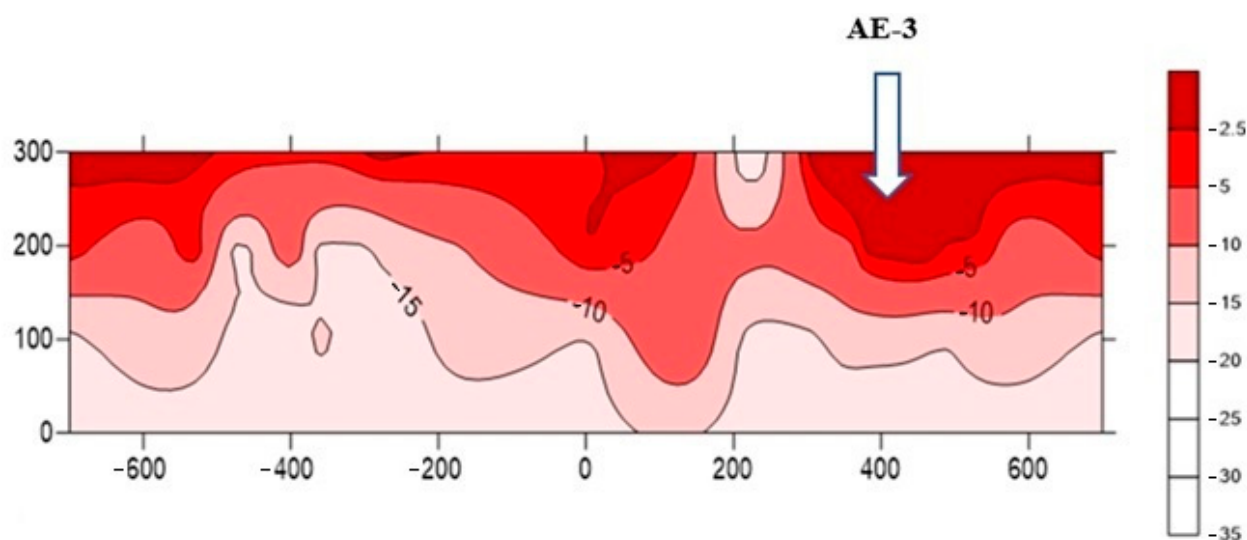


**Figure 9.** Map for the ADC descriptor values on the side walls of the tank of the tested transformer T1 after 1.5 h of supply by  $1.7 U_R$  voltage within the frequency band from 110 kHz to 200 kHz. Coordinates (X,Y) of the transformer tank points as described in Figure 7.

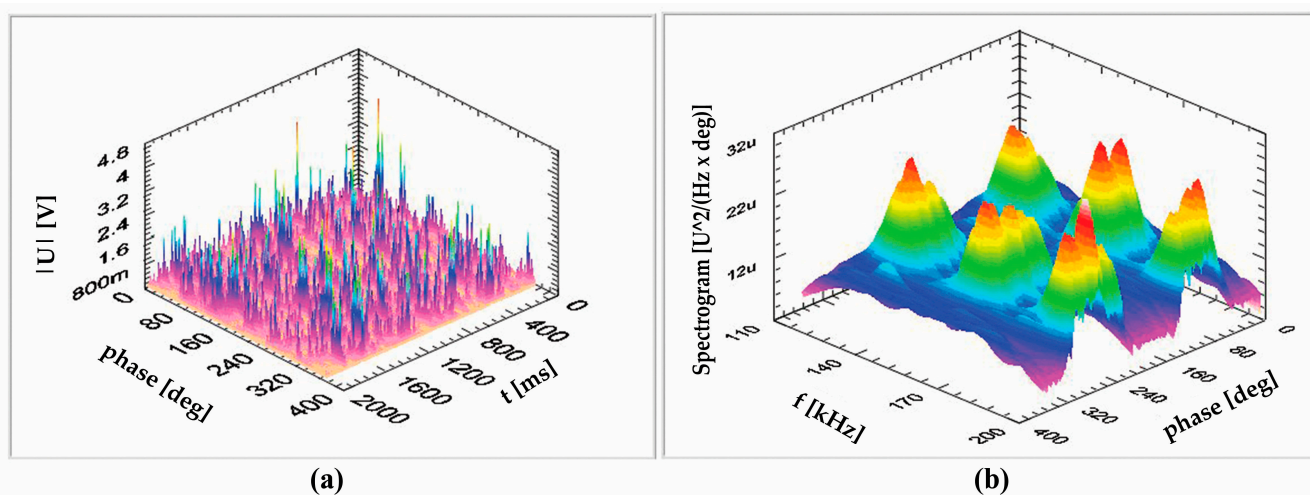


**Figure 10.** Acoustic image of a selected AE signal from AE-3 area within the Figure 9: (a) amplitude-phase-time characteristics, (b) averaged three-dimensional STFT spectrogram. AE signal parameters: ADC =  $-0.56$ ,  $U_{PP} = 7.85$  V,  $U_{rms} = 166.74$  mV.

The results of the PD tests in the T1 transformer carried out in parallel with the electrical and AE methods confirm the correctness of the authors' proposed AE method. Measurements by the electrical method give the apparent charge measured introduced by all PD sources existing within each phase of the transformer. The descriptor maps on the sidewalls of the transformer tank locate the PD sources.

Figure 7 shows the lack of PDs sources in the L1 phase and single PD sources in the L2 and L3 phases located in the areas AE-1 and AE-2. The recorded AE signals have very small ADC descriptors. This shows agreement with the electrical method test results.

On the other hand, the results of electrical tests for a voltage of  $1.7 U_R$  after more than 1.5 h from the application of the supply voltage give an apparent charge of 1 nC in each of the phases. The description of the test results using the AE method shown in Figure 9 shows that signals with large or very large descriptor values are recorded on large areas of the side walls of the transformer tank. This indicates that there are numerous sources of PDs in the transformer. The detailed analysis presented here gives an identification of the source types and forms the basis of the diagnosis made.



The accuracy of this diagnosis was positively verified during the revision of the transformer and became the starting point for PD testing using the authors' AE method in subsequent transformers during their ongoing operation.

#### 4.3. AE Testing during Ongoing In-Situ Operation

PD tests were carried out in two oil power transformers of identical design during their ongoing in-situ operation. These are transformers with transformer ratio of 120/20/6 kV and a rated power of 25 MVA. The transformers have extremely different service histories. The operation of one of them, in this paper called T2, proceeded smoothly. During the operation of the second of them, in this work called T3, spontaneous shutdown occurred several times due to the tripping of the Buchholz protection, and several times overheating was detected in post-failure tests. The results of the analysis of the recorded signals are presented in Figures 11–16, respectively.

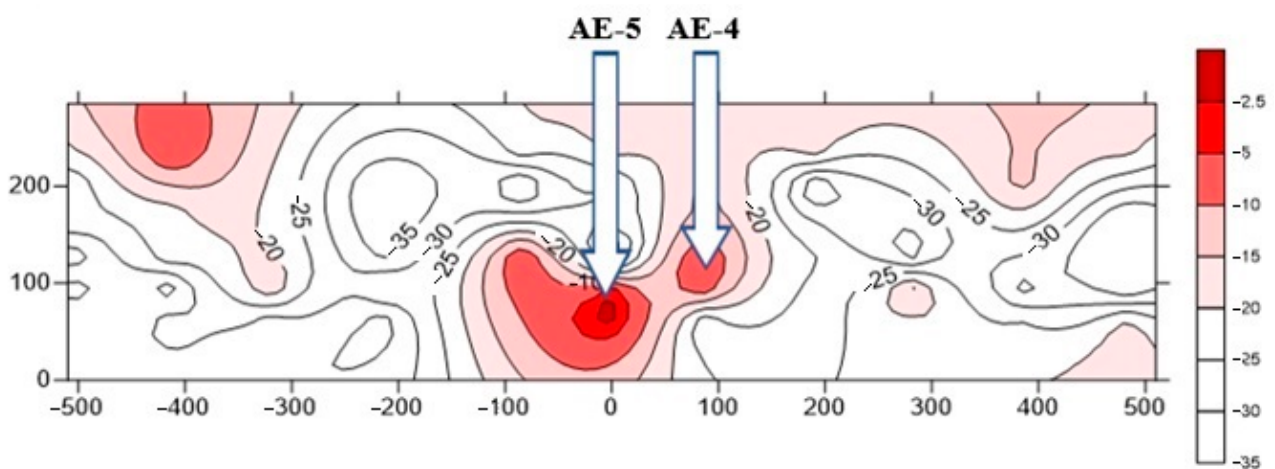


**Figure 11.** Map for the ADC descriptor values on the lateral walls of the tank of the tested transformer T2 within the frequency band from 110 kHz to 200 kHz. Coordinates (X,Y) of the transformer tank points as described in Figure 7.

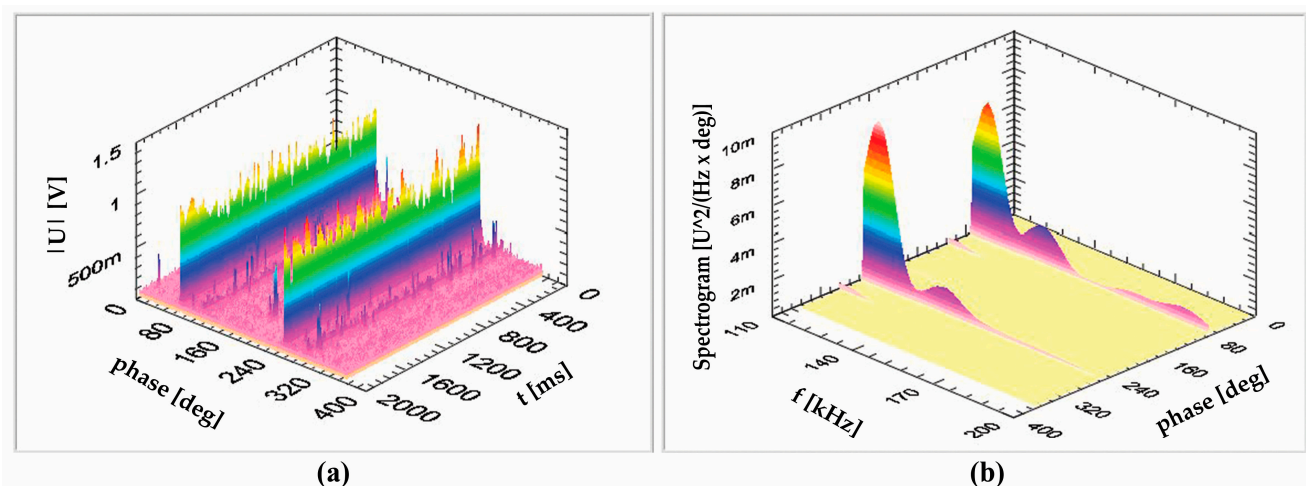


**Figure 12.** Acoustic image of a selected AE signal from AE-4 area within the Figure 11: (a) amplitude-phase-time characteristics, (b) averaged three-dimensional STFT spectrogram. AE signal parameters: ADC =  $-2.96$ ,  $U_{pp} = 2.91$  V,  $U_{rms} = 61.89$  mV.

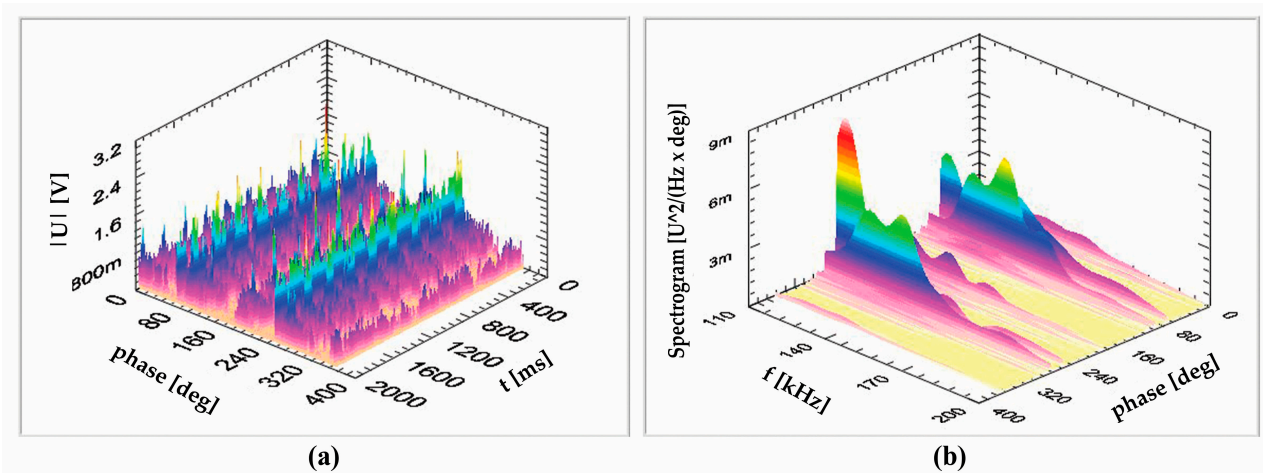


**Figure 13.** Acoustic image of a selected AE signal from AE-5 area within the Figure 11: (a) amplitude-phase-time characteristics, (b) averaged three-dimensional STFT spectrogram. AE signal parameters: ADC = -1.74,  $U_{pp} = 5.60$  V,  $U_{rms} = 128.50$  mV.

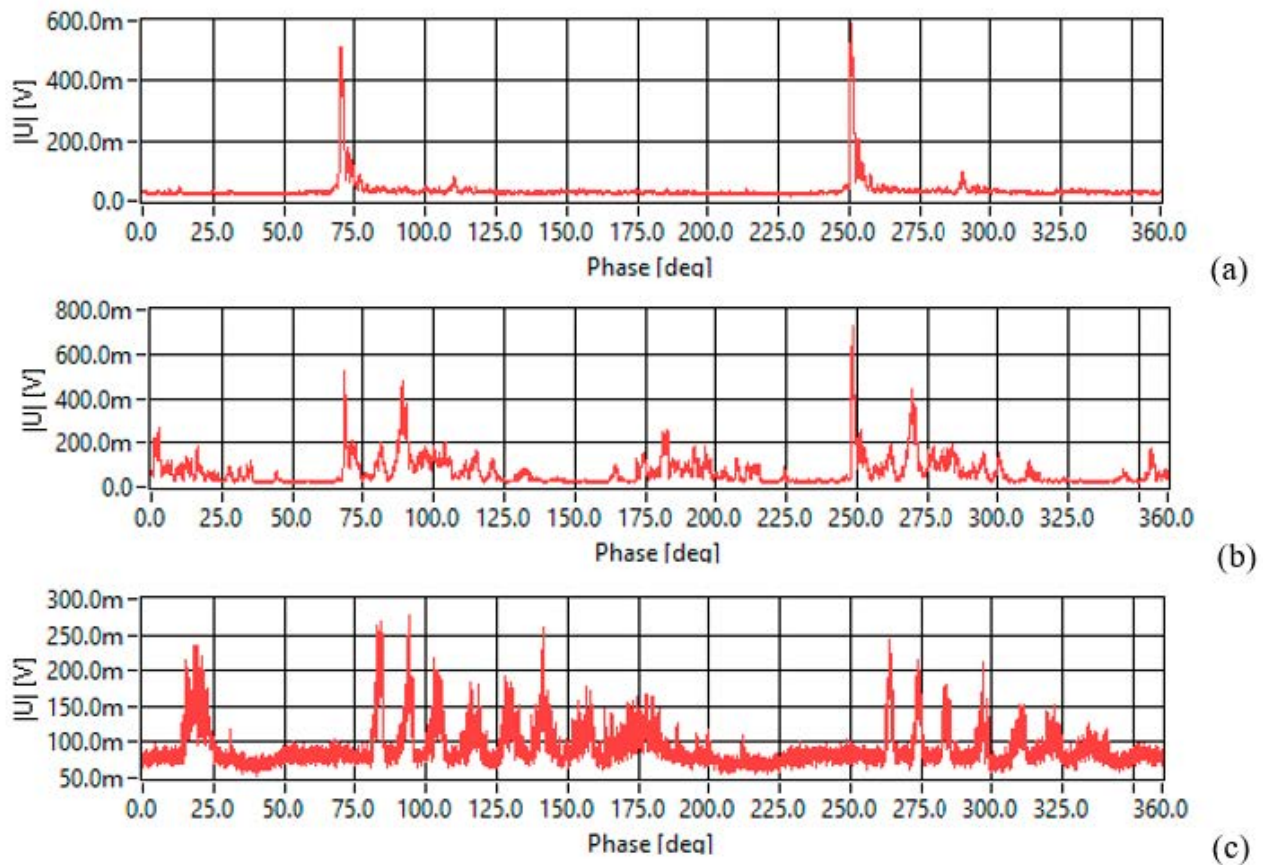


**Figure 14.** Averaged amplitude-phase characteristics for signals from: (a) Figure 12, (b) Figure 13, (c) Figure 16.

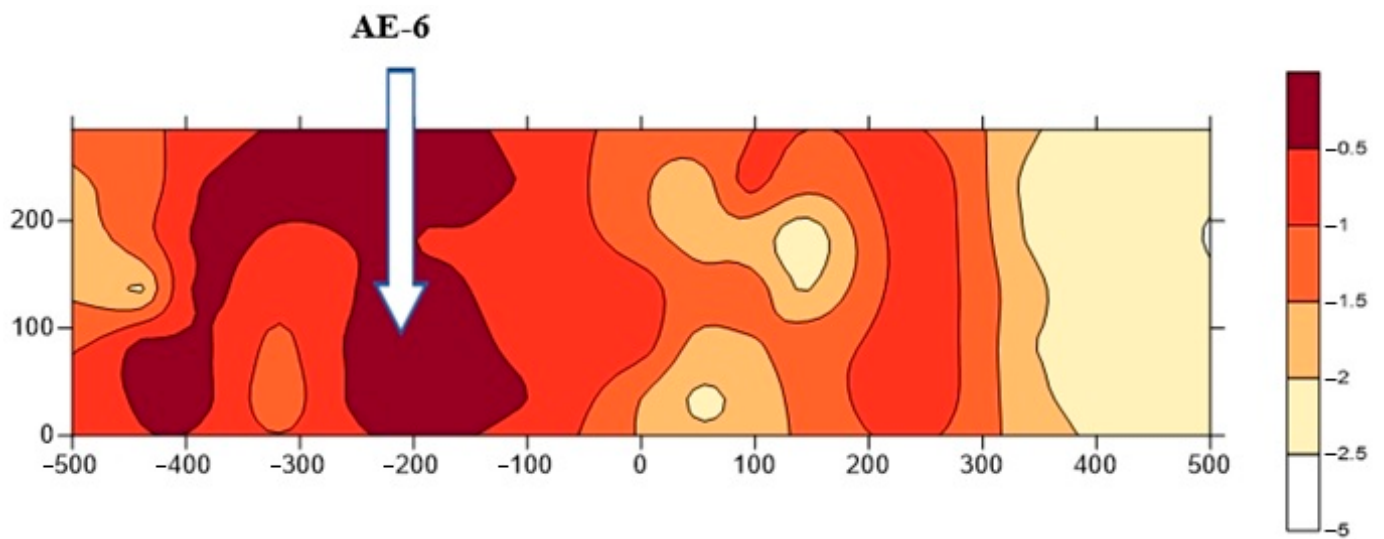


**Figure 15.** Map for the ADC descriptor values on the lateral walls of the tank of the tested transformer T3 within the frequency band from 110 kHz to 200 kHz. Coordinates (X,Y) of the transformer tank points as described in Figure 7.

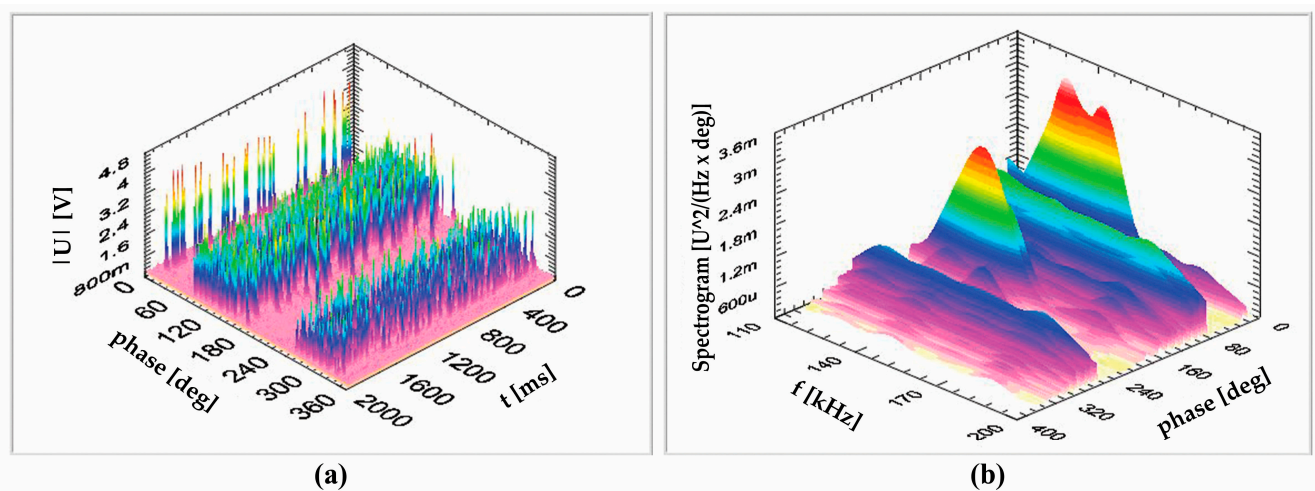


**Figure 16.** Acoustic image of a selected AE signal from AE-6 area within the Figure 15: (a) amplitude-phase-time characteristics, (b) averaged three-dimensional STFT spectrogram. AE signal parameters: ADC =  $-0.29$ ,  $U_{pp} = 8.28$  V,  $U_{rms} = 163.06$  mV.

The ADC descriptor map for the T2 transformer (Figure 11) gives the location of the most active PDs in the region AE-5, located in the TC. The second region AE-4 is also located in the TC, in which there are PDs with lower ADC descriptor values. Figures 12 and 13 show the characteristics giving acoustic images of the signals recorded in these areas. In the AE-4 area, the signals are well located in phase (signals appearing at the supply voltage phases of approximately  $75^\circ$  and  $250^\circ$  dominate). The signals occurring in the AE-5 area, where the most active PDs occur, have maximum values for identical supply voltage phase values, but there are also signals for other phase values. A comparison of the averaged amplitude-phase characteristics for these signals presented in Figure 14a,b shows the similarity of the mechanisms of generating these signals. This location of PDs gives information about PDs generated in the TC and can be checked and verified in future revisions. For the operation of the transformer, the condition of the winding insulation is the most important. Since the tests carried out do not show the occurrence of PDs in the insulation areas of the windings, a positive diagnosis of the insulation condition of the windings and no obstacles to the further operation of transformer T2 is made.

The ADC descriptor map for the T3 transformer presented in Figure 15 shows the occurrence of PDs with very high activity in many areas of the transformer. In particular, it is a large area marked AE-5 located on the low voltage bushing side (LVbs). It entirely includes the area where the winding for the L1 phase occurs and partially includes the areas where the windings for L2 and L3 phases occur. The acoustic image of the exemplary signal recorded in the AE-5 area shown in Figures 16 and 14c confirms the occurrence of very advanced PDs.

As the investigations carried out show the presence of very advanced PDs in the winding insulation areas, the authors make a negative diagnosis of the winding insulation condition along with a suggestion to refer the transformer for overhaul (visual inspection of the windings and core).

The owner of transformer T3, taking into account the diagnosis made and previous incidents occurring during the operation of the transformer, decided to carry out an overhaul. During the overhaul, after a visual inspection, a new core and new windings were made.

The subject of further research was an oil power transformer with a rated voltage of 110 kV and a power of 25 MVA. The tests were carried out in the fifth year of its operation. The reason for conducting the tests using the AE method were the results of several tests of the transformer oil using the Dissolved Gas Analysis (DGA) chromatographic analysis method. The DGA tests show the presence of hydrogen in the oil, and in addition the level of hydrogen found in successive tests was increasing. These facts clearly indicate the occurrence of PDs in the transformer.

PD tests were carried out using the AE method in this transformer (in this work, named as T4). The ADC descriptor map for the T4 transformer precisely locates the one area where signals with very high ADC descriptor values are registered. This area is between the TC and the L1 winding and is outside the areas of the transformer windings. The authors make a diagnosis of the presence of advanced PD sources in this area and recommend a revision of this area.

The conducted revision shows that in this area, the wire connecting winding in phase L1 with tap changer had slipped out of the mounts and was very close to the transformer tank. Such a location of the wire became a source of PD with very high activity. The proper installation of the cable was restored and subsequent tests of the transformer oil by the DGA method did not reveal the presence of hydrogen. Such a result means, therefore, no PDs.

## 5. Conclusions

The authors' multi-channel acoustic emission DEMA-COMP and 8AE-PD measurement systems dedicated to study the phenomena of PDs arising in dielectrics or electroenergetic devices within an alternating electric field are presented.

Both systems enable the monitoring of signals in the selected measurement channel, simultaneous recording of signals in all measurement channels in real time, providing in each measurement channel a bandwidth of 20–500 kHz (DEMA-COMP) or 20–1000 kHz (8AE-PD) and the analysis of the recorded signals.

As the result of the research, the following features are selected to describe the recorded AE signals: maximum amplitude, minimum amplitude, energy of signal, frequency bands and phase bands characteristic of the signal and the ADC descriptor, which ranks the signals according to the so-called degree of advancement.

It has been shown that for single sources of PDs, the ordering of the registered signals by the ADC descriptor coincides with the ordering by the values of the apparent charge introduced by the single sources. This descriptor property is the basis for calibrating the results of the AE method with the results of the electrical method.

This study demonstrates the functionality of both measurement systems under laboratory conditions and during ongoing in-situ operation of power oil transformers.



The authors' patented method of PDs' location and identification in power oil transformers together with the results of tests carried out on four selected objects are presented (one at the test station, three during ongoing in-situ operation).

Tests of the transformer at the test station, aimed at verifying the AE method, show the compatibility of the results obtained with the AE method and the electrical method.

Based on the results obtained from the PDs in power oil transformers using the AE method, the authors make diagnoses of the condition of the insulating systems of the examined transformers. These diagnoses require revision (2 cases) or repair (1 case) of the transformer. The owners of these transformers have performed the respective revisions and repairs. In all cases, the actions of the owners confirm the accuracy of the localization and identification of PDs performed by the authors.

**Author Contributions:** Conceptualization, F.W.; methodology, F.W.; software, F.W. and A.O.; validation, F.W. and A.O.; formal analysis, F.W. and A.O.; investigation, F.W. and A.O.; resources, F.W.; data curation, F.W. and A.O.; writing—original draft preparation, F.W.; writing—review and editing, F.W. and A.O.; visualization, F.W. and A.O.; supervision, F.W. All authors have read and agreed to the published version of the manuscript.

**Funding:** This research received no external funding.

**Institutional Review Board Statement:** Not applicable.

**Informed Consent Statement:** Not applicable.

**Data Availability Statement:** Not applicable.

**Conflicts of Interest:** The authors declare no conflict of interest.

## References

1. Wong, J.K.R.; Illias, H.A.; Bakar, A.H.A.; Mokhlis, H. Partial discharge classifications: Review of recent progress. *Measurement* **2015**, *68*, 164–181.
2. Rodrigo Mor, A.; Castro Heredia, L.C.; Harmsen, D.A.; Muñoz, F.A. A new design of a test platform for testing multiple partial discharge sources. *Int. J. Electr. Power Energy Syst.* **2018**, *94*, 374–384. [[CrossRef](#)]
3. Hussain, M.R.; Refaat, S.S.; Abu-Rub, H. Overview and Partial Discharge Analysis of Power Transformers: A Literature Review. *IEEE Access* **2021**, *9*, 64587–64605. [[CrossRef](#)]
4. Callender, G.; Lewin, P.L. Modeling partial discharge phenomena. *IEEE Electr. Insul. Mag.* **2020**, *36*, 29–36. [[CrossRef](#)]
5. Faiz, J.; Soleimani, M. Dissolved gas analysis evaluation in electric power transformers using conventional methods a review. *IEEE Trans. Dielectr. Electr. Insul.* **2017**, *24*, 1239–1248. [[CrossRef](#)]
6. Shang, H.; Xu, J.; Zheng, Z.; Qi, B.; Zhang, L. A Novel Fault Diagnosis Method for Power Transformer Based on Dissolved Gas Analysis Using Hypersphere Multiclass Support Vector Machine and Improved D–S Evidence Theory. *Energies* **2019**, *12*, 4017. [[CrossRef](#)]
7. Ilkhechi, H.D.; Samimi, M.H. Applications of the Acoustic Method in Partial Discharge Measurement: A Review. *IEEE Trans. Dielectr. Electr. Insul.* **2021**, *28*, 42–51. [[CrossRef](#)]
8. Boczar, T.; Borucki, S.; Jancarczyk, D.; Bernas, M.; Kurtasz, P. Application of Selected Machine Learning Techniques for Identification of Basic Classes of Partial Discharges Occurring in Paper-Oil Insulation Measured by Acoustic Emission Technique. *Energies* **2022**, *15*, 5013. [[CrossRef](#)]
9. Shanker, T.B.; Nagamani, H.N.; Antony, D.; Punekar, G.S. Effects of Transformer-Oil Temperature on Amplitude and Peak Frequency of Partial Discharge Acoustic Signals. *IEEE Trans. Power Deliv.* **2018**, *33*, 3227–3229. [[CrossRef](#)]
10. Búa-Núñez, I.; Posada-Román, J.E.; Rubio-Serrano, J.; Garcia-Souto, J.A. Instrumentation System for Location of Partial Discharges Using Acoustic Detection with Piezoelectric Transducers and Optical Fiber Sensors. *IEEE Trans. Instrum. Meas.* **2014**, *63*, 1002–1013. [[CrossRef](#)]
11. Besharatifard, H.; Hasanzadeh, S.; Heydarian-Forushani, E.; Alhelou, H.H.; Siano, P. Detection and Analysis of Partial Discharges in Oil-Immersed Power Transformers Using Low-Cost Acoustic Sensors. *Appl. Sci.* **2022**, *12*, 3010. [[CrossRef](#)]
12. Sikorski, W.; Walczak, K.; Gil, W.; Szymczak, C. On-Line Partial Discharge Monitoring System for Power Transformers Based on the Simultaneous Detection of High Frequency, Ultra-High Frequency, and Acoustic Emission Signals. *Energies* **2020**, *13*, 3271. [[CrossRef](#)]
13. Sikorski, W. Development of Acoustic Emission Sensor Optimized for Partial Discharge Monitoring in Power Transformers. *Sensors* **2019**, *19*, 1865. [[CrossRef](#)]
14. Secic, A.; Krpan, M.; Kuzle, I. Vibro-Acoustic Methods in the Condition Assessment of Power Transformers: A Survey. *IEEE Access* **2019**, *7*, 83915–83931. [[CrossRef](#)]



15. Kunicki, M.; Wotzka, D. A Classification Method for Select Defects in Power Transformers Based on the Acoustic Signals. *Sensors* **2019**, *19*, 5212. [[CrossRef](#)]
16. Rocío, N.A.M.; Nicolás, N.; Isabel, L.P.M.; José, R.; Linilson, P. Magnetic Barkhausen Noise and Magneto Acoustic Emission in Stainless Steel Plates. *Procedia Mater. Sci.* **2015**, *8*, 674–682. [[CrossRef](#)]
17. Makowska, K.; Piotrowski, L.; Kowalewski, Z.L. Prediction of the Mechanical Properties of P91 Steel by Means of Magneto-acoustic Emission and Acoustic Birefringence. *J. Nondestruct. Eval.* **2017**, *36*, 43. [[CrossRef](#)]
18. Kunicki, M. Analysis on Acoustic Disturbance Signals Expected during Partial Discharge Measurements in Power Transformers. *Arch. Acoust.* **2020**, *45*, 733–746.
19. Borucki, S.; Cichoń, A.; Majchrzak, H.; Zmarzły, D. Evaluation of the Technical Condition of the Active Part of the High Power Transformer Based on Measurements and Analysis of Vibroacoustic Signals. *Arch. Acoust.* **2017**, *42*, 313–320. [[CrossRef](#)]
20. Witos, F.; Opilski, Z.; Szerszeń, G.; Setkiewicz, M. The 8AE-PD computer measurement system for registration and analysis of acoustic emission signals generated by partial discharges in oil power transformer. *Metrol. Meas. Syst.* **2019**, *26*, 404–418.
21. Witos, F.; Opilski, Z.; Szerszeń, G.; Setkiewicz, M.; Olszewska, A.; Duda, D.; Maźniewski, K.; Szadkowski, M. Calibration and laboratory testing of computer measuring system 8AE-PD dedicated for analysis of acoustic emission signals generated by partial discharges within oil power transformers. *Arch. Acoust.* **2017**, *42*, 297–311. [[CrossRef](#)]
22. Witos, F.; Szerszeń, G.; Setkiewicz, M. Mounting Magnetic Holders, Especially for Acoustic Emission Sensors, to the Side Surfaces of the Transformer Tank. PL Patent 223606 B1, 31 October 2016. (In Polish)
23. Shie, Q.; Dapang, C. Joint time-frequency analysis. *IEEE Signal Process. Mag.* **1999**, *16*, 52–67. [[CrossRef](#)]
24. Muir, C.; Swaminathan, B.; Almansour, A.S.; Sevener, K.; Smith, C.; Presby, M.; Kiser, J.D.; Pollock, T.M.; Daly, S. Damage mechanism identification in composites via machine learning and acoustic emission. *Comput. Mater.* **2021**, *7*, 95–119. [[CrossRef](#)]
25. IEC 60270:2000; High-Voltage Test Techniques—Partial Discharge Measurements. International Standards: London, UK, 2000.
26. Witos, F.; Opilski, Z. The Method of Partial Discharges Locating, Particularly in the Power Oil Transformers, Based on the Map of Acoustic Emission Descriptors in the Frequency. Domain. Patent PL 223605 B1, 31 October 2016. (In Polish)
27. EN 14584:2013-07; Non-Destructive Testing—Acoustic Emission Testing—Examination of Metallic Pressure Equipment During Proof Testing—Planar Location of AE Sources. European Committee for Standardization: Brussels, Belgium, 2013.
28. Witos, F.; Olszewska, A.; Opilski, Z.; Lisowska-Lis, A.; Szerszeń, G. Application of acoustic emission and thermal imaging to test oil power transformers. *Energies* **2020**, *13*, 5955. [[CrossRef](#)]

**Disclaimer/Publisher’s Note:** The statements, opinions and data contained in all publications are solely those of the individual author(s) and contributor(s) and not of MDPI and/or the editor(s). MDPI and/or the editor(s) disclaim responsibility for any injury to people or property resulting from any ideas, methods, instructions or products referred to in the content.